Uptake, accumulation, and translocation of Zn, Cu, Pb, Cd, Ni, and Cr by *P. australis* seedlings in an urban dredged sediment mesocosm: Impact of seedling origin and initial trace metal content

Nicole Nawrot [a,*], Ewa Wojciechowska [a], Ksenia Pazdro [b], Jacek Szmagliński [a], Janusz Pempkowiak [c]

[a] *Gdańsk University of Technology, Faculty of Civil and Environmental Engineering, Narutowicza 11/12, 80-233 Gdańsk, Poland*
[b] *Institute of Oceanology of the Polish Academy of Sciences, Marine Geotoxicology Laboratory, Powstańców Warszawy 55, 81-712 Sopot, Poland*
[c] *Institute of Oceanology of the Polish Academy of Sciences, Marine Biogeochemistry Laboratory, Powstańców Warszawy 55, 81-712 Sopot, Poland*

HIGHLIGHTS

- Initial body content of trace metals in *P. australis* is crucial for phytoremediation.
- Uptake of trace metals by seedling with low initial content.
- Release of trace metals by seedlings with initial high metal content.
- Dredged sediments pH and high mineral matter content can limit biomass growth.
- Disturbance of cortical cells and deformation of aerenchyma as plant stress reply.

GRAPHICAL ABSTRACT
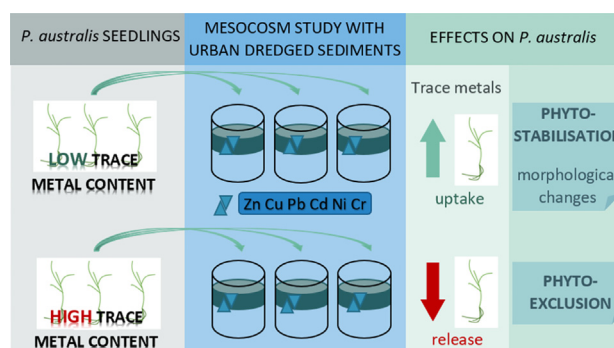
ABSTRACT

The study presents results from 6 months of phytoremediation of sediments dredged from three urban retention tanks carried out in a mesocosm setup with the use of *P. australis*. Two kinds of *P. australis* seedlings were considered: seedlings originating from natural (uncontaminated - S_{uncont}) and anthropogenically changed environments (contaminated – S_{cont}); this distinction was reflected in the baseline concentrations of trace metals inside their tissues. The potentially toxic elements (PTEs) considered in this study were as follows: Zn, Cu, Cd, Ni, Cr, and Pb. The aim of the study was to compare the uptake, accumulation, and translocation properties of seedlings with different initial trace metal contents. The PTE concentrations were analyzed in sediments as well as in belowground and aboveground parts of plants in the middle (3rd month) and at the end of the investigation period using inductively coupled plasma mass spectrometry (ICP-MS), and the accumulation of PTEs in plant tissues was calculated. Phytoextraction efficiency was evaluated using the bioconcentration factor (BF) and translocation factor (TF). Plant morphology was assessed with scanning electron microscopy (SEM) to document plant stress due to PTE exposure. The results of our study indicated that *P. australis* seedlings originating from sites differing in the initial trace metal content exhibited different behavior when grown on sediments dredged from urban retention tanks. S_{uncont} seedlings with low initial metal contents tended to adapt to the dredged sediments and showed phytoextraction ability, while S_{cont} seedlings originating from sites with initial high contents of trace metals acted as phytoexcluders and tended to release PTEs from their tissues into the sediments. The morphological and structural effects caused by metal toxicity were observed in growth limitation, root tissue disturbance, root hair number decrease, and structural alterations in the epidermis and endodermis. Therefore, the S_{uncont} seedlings presented better properties and adaptability for phytoremediation purposes.

* Corresponding author.
E-mail address: nicnawro@pg.edu.pl (N. Nawrot).

1. Introduction

For almost five decades, *P. australis* (common reed) has been frequently used for phytoremediation of contaminated water, soil, and sediment (Rezania et al., 2019). This species is classified as an emergent macrophyte, while other species exhibit floating-leaf, submerged, or free-floating life forms (Shaltout et al., 2006). There is valid interest in the mechanisms regulating the growth and distribution of *P. australis* due to the constant interest in wetland construction and restoration for wildlife, water treatment and sustainable urban architecture according to the green infrastructure approach. *P. australis* is a common species that is widespread on almost all continents. Its habitat includes climate zones ranging from cool to tropical and arid. For all European countries, this species is recognized as native (Packer et al., 2017). *P. australis* demonstrates high plasticity and the ability to adapt to a broad range of environmental conditions (Milke et al., 2020), especially in the context of potentially toxic elements (PTEs), which are mostly represented by metals (Cd, Co, Cr, Cu, Fe, Hg, Mn, Mo, Ni, Pb, Sn, V, and Zn), metalloids (As, Sb), and nonmetals (Se) (Antoniadis et al., 2021; Shaheen et al., 2019). Based on the data provided by Packer et al. (2017), *P. australis* occurs in its native range globally under the following substrate conditions (in min-max ranges): N (0–2430 mg/kg), P (180–6890 mg/kg), Cd (<44 mg/kg), Pb (<15,900 mg/kg), Cu (<275 mg/kg d.w.), Cr (<218 mg/kg d.w.), Zn (<11,000 mg/kg d.w.), and Ni (<81.6 mg/kg). In Europe, the pH of the solid substrate in which *P. australis* grows is generally 7; however, populations thrive when the pH is between 5.5 and 7.5. The successful development of *P. australis* is also limited by the water table and light (Shaltout et al., 2006). Common reeds have the ability to take up high levels of trace metals due to their expanded tissue system and defense mechanisms (Huang et al., 2018; Obarska-Pempkowiak et al., 2015). The presence of aerenchyma in the roots and rhizomes plays a vital role in the improvement of anaerobic conditions and associated biogeochemical processes in sediments. In general, mechanisms of purification performed by macrophytes encompass nutrient uptake, biofilm development, extracellular enzyme release, contaminant settling and binding in addition to metal redistribution (Yeh et al., 2015). *P. australis* contains a high amount of lignin and cellulose, which adsorb significant quantities of trace elements from aqueous solutions and solid phases including sediment and soil (Shi et al., 2018). The translocation of trace metals to different parts of *P. australis* has been widely studied, with the highest element concentrations in the following order: roots, rhizomes, leaves, and stems (Al-Homaidan et al., 2020). Some authors (Corzo Remigio et al., 2020; Wojciechowska and Waara, 2011) proved that uptake is most intensive in the early stage of the vegetative period. Colonies are generally propagated vegetatively (but also through seeds) and expand peripherally by lateral rhizome growth, which is typically subterranean. Vegetative propagation is useful for solid material conservation and the stabilization of sediments (Shaltout et al., 2006).

Concerning urban districts, the introduction of potentially toxic elements (PTEs) to the surrounding environment (soil, sediment, and water) remains a valid concern and poses serious environmental and health risks. Thus, it is ecologically justified to consider the abilities of common reed for the treatment of sediments affected by PTEs. Sediments deposited in urban stormwater drainage systems (including streams and rivers flowing through cities as well as urban retention ponds) constitute a specific sink for contaminants. Through the influence of different pathways, such as highway traffic, fossil fuel combustion, and industrial production, airborne pollutants are deposited onto impermeable surfaces during the dry period (Murphy et al., 2015; Nawrot et al., 2020a). They are subsequently washed away by surface runoff, which affects the quality of stormwater receivers (Nawrot and Wojciechowska, 2018). Trace elements entering the aquatic ecosystem are associated with the fine-grained fraction of sediments and suspended solids due to their large surface areas and high sorption capacities (Bednarova et al., 2013). Throughout the hydrological cycle, 99% of trace metals are stored in sediments,

which, therefore, are the major sinks and carriers for contaminants in aquatic environments (Bartoli et al., 2012). Far less than 1% of PTEs remain dissolved in water; the water quality is, therefore, a temporary reflection of environmental contamination status (Omwene et al., 2018), while sediments are the ultimate repository reflecting long-term changes. During the last 20 years, the approach to contaminated sediment management changed from storage in confined disposal facilities to the use of phytotechnology and revitalization in situ. The volumes estimated by SedNet (European Sediment Network) indicate that approximately 100–200 million cubic meters of contaminated sediments might be produced yearly in Europe. Moreover, urban sediments have specific characteristics, including a high content of mineral matter and little organic matter; therefore, their use as organic raw materials is completely out of question. In addition to trace metal loading, they may contain other hazardous substances, such as polycyclic aromatic hydrocarbons (PAHs). Due to the large scale of the problem and the large volume of sediments formed, European policy encourages sediment valorization (Achour et al., 2014). The sustainable approach included in the "best management practices" noted phytoremediation as an alternative to technologically advanced methods (Rezania et al., 2016). This strategy is also in line with the approaches defined in the UN Sustainable Development Goals 13 (climate action) and 15 (life on land). Due to the low costs, simple operation, and efficiency of macrophytes for phytoextraction, numerous phytoremediation feasibility studies have focused on the treatment of sediments contaminated with toxic elements (Cicero-Fernández et al., 2017; Sarwar et al., 2017). Moreover, this approach can be integrated quite intuitively into the existing water infrastructure inside cities, which relies on the use of hydrophytes with specific PTE absorbing abilities, e.g., native *P. australis*.

To the best of our knowledge, the properties of *P. australis* seedlings and their original metal content in the context of metal uptake, accumulation, and translocation at the first stage of growth as well as their responses to dredged sediment exposure have not been studied thus far. The successful use of green technologies requires thorough investment and efficiency analyses. Plants have to be able to grow on the site and "work" at the desired level, which can sometimes be disturbed. Therefore, a mesocosm study with *P. australis* seedlings (with different places of origin and initial trace metal contents including those of Zn, Cu, Pb, Cd, Ni, and Cr) planted in urban dredged sediments in batch reactors was performed to gain information on trace metal redistribution on plant-sediment borders. Two types of seedlings were tested: (1) those originating from a natural environment (uncontaminated) and (2) those originating from an anthropogenically changed (contaminated) environment where the exposure of PTEs in the initial stage of growth occurred at diverse levels. Trace metals were analyzed in the belowground and aboveground parts of *P. australis*. The toxic effects of Zn, Cu, Pb, Ni, Cr, and Cd in *P. australis* were determined by analysis of the structural changes in tissues (roots & rhizomes). The main research question stated under this study is whether different initial contents of trace metals in vegetative seedlings of common reed affect the uptake of metals from dredged sediment substrates. Moreover, whether seedlings showed the ability to adapt and grow on dredged sediments and how this environment affected their status in terms of morphological and anatomical changes was investigated. A side topic of this study is the effect of sediment phytoremediation.

2. Materials & methods

2.1. Laboratory set-up

A series of batch mesocosm experiments were conducted between April and September 2018. The mesocosm phytoremediation setup (Fig. 1) consisted of 2 configurations of 3 columns of a 0.6 m³ volume. Each column was equipped with a drainage system comprising the following (from the bottom): an outlet protected by stones (32–60 mm), 20 cm drainage layer of stones (16–32 mm), 20 cm drainage layer of
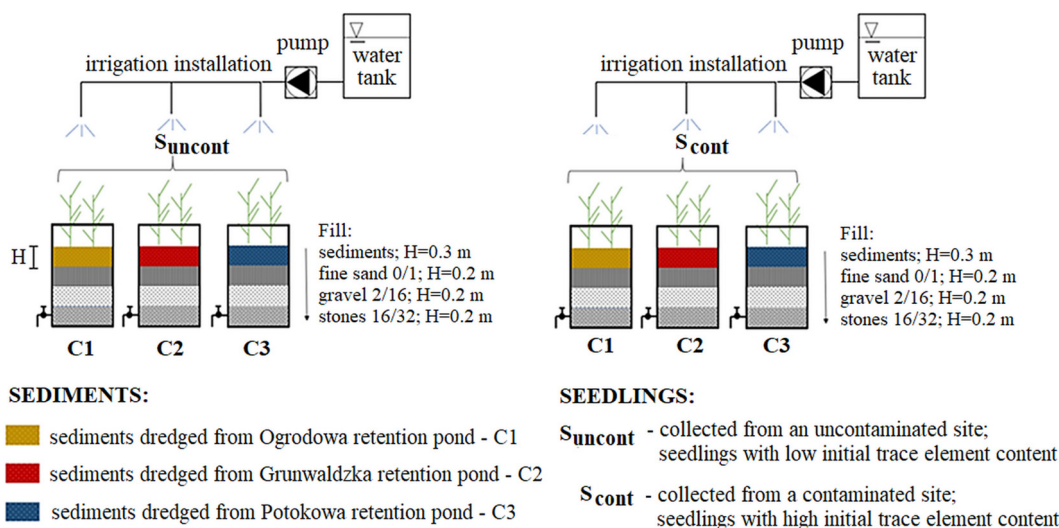
Fig. 1. Scheme of the mesocosm system for phytoremediation analysis with the use of *P. australis* seedlings with different origins and initial contents of trace metals: S_{uncont} (collected from uncontaminated site) and S_{cont} (collected from contaminated site) on diverse sediments dredged from urban open stormwater retention ponds; Column 1 (C1) – sediments extracted from Ogrodowa, Column 2 (C2) – sediments extracted from Grunwaldzka, and Column 3 (C3) – sediments extracted from Potokowa retention ponds.

gravel (2–16 mm), 20 cm drainage layer of fine sand (0.1 mm) and 30 cm layer of tested dredged sediments. Dredged sediments were collected in March 2018 from three open stormwater retention ponds (which are the receivers for stormwater runoff) (Ogrodowa 54°22′12.2″N 18°34′20.0″E, Grunwaldzka 54°24′46.4″N 18°34′02.9″E, and Potokowa 54°22′28.3″N 18°34′09.6″E retention ponds) located on the two longest streams in Gdansk – the Strzyza and Oliwski streams -and placed in the mesocosm setup. From each retention pond, a volume of 0.5 m³ of wet sediments was dredged, mixed, and homogenized. Then, a volume of 0.15 m³ of representative sediments was used in the mesocosm as a top layer (where *P. australis* seedlings were planted), and representative subsamples of sediments were collected in PE bags for further chemical analyses, allowing us to determine the trace metal contents in the dredged sediments. Ultimately, the mesocosm setup consisted of 2 sets of 3 columns with diverse dredged sediments used as a surface layer in each batch reactor (dredged sediment arrangement: C1- sediments from Ogrodowa, C2- sediments from Grunwaldzka, and C3- sediments from Potokowa retention ponds). These dredged sediments were chosen due to their high trace element content detected in urban open stormwater retention ponds in Gdansk in previous studies by (Nawrot et al., 2020b; Wojciechowska et al., 2017, 2019).

P. australis seedlings (3–4 seedlings) were planted in each column after harvest from their original site. The seedlings were collected in the 2nd half of April 2018, which means that at the time of their collection, the seedlings at the original site had shown active growth (the early vegetation period in 2018) for approx. 2–3 weeks since the vegetation period in northern Poland starts no sooner than April. Two different sampling points were chosen for collection purposes– the natural lake edge hereinafter referred to as the uncontaminated seedling sampling site (seedlings marked as S_{uncont}) and along the roadside ditch further referred to as the contaminated site (seedlings marked as S_{cont}). In this study, seedlings were distinguished by an index referring to the place of origin (S_{uncont} and S_{cont}), which was also connected with different initial trace metal contents inside their tissues, as presented in Table 1. The analyzed trace elements in plants and sediments included Cu, Zn, Pb, Cd, Ni, and Cr. In both locations, along with the 80–100 m distance, 10–12 samples for the mesocosm setup, 4 samples for chemical composition testing and 2 control samples (CONTROL) of *P. australis* seedlings were collected within a 5×2 m² plot (as shown in Fig. S.1). Vegetative seedlings of different clones were sampled. Seedling collection, preparation, and initial trace metal analyses were performed according to Nawrot et al. (2019). Seedlings were transported in water

and taken to the laboratory within 1 h after extraction. Immediately, seedlings of *P. australis* were cleaned using Milli-Q water and planted in the mesocosm setup. The representative group of seedling samples for chemical composition assessment at the beginning of the experiment was determined according to section 2.2.1.

Under the mesocosm configuration, the first set of 3 columns was planted with S_{uncont}, and the second set of 3 columns was planted with S_{cont}. The set ups were equipped with a 10 L water tank, irrigation, and a pump to maintain a constant water level in each column (the water level was maintained 2 cm above the surface of the sediments). The outflows were protected by ball valves. Tap water used to supplement the experimental setups corresponded to the following metal contents: Pb < 10 µg/L, Cu < 2 mg/L, Cd < 5 µg/L, Cr < 50 µg/L, and Ni < 20 µg/L. Every week, the water level was checked and supplemented if needed. No additional fertilization was carried out. Plant growth was determined by a measuring tape in one-week intervals. The experiment lasted for almost 6 months and covered almost the entire vegetation season for *P. australis* in Poland. Seedling samples were collected at the middle (June 2018) and end (September 2018) of the experiment for chemical analyses. In the case of sediments, the trace metal concentration was checked at the end of the experiment. In the middle and at the end of the experiment, S_{uncont} (from column C3, where the appearance of reeds indicated the stress caused by sediment toxicity) was collected for scanning electron microscopy (SEM) analysis. The biomasses of harvested seedlings of S_{uncont} and S_{cont} at the end of the mesocosm experiment are presented in Table S.1.

2.2. Chemical analyses of trace metals

2.2.1. P. australis

Samples of *P. australis* for chemical analyses were preliminarily cleaned using Milli-Q water and separated into roots and rhizomes (BG - belowground parts), stems (ST), and leaves (LF). The sorted plant tissues were placed in Petri dishes and lyophilized to a constant weight. After that, plant organs were weighed and ground in a mill (Millix 20) and processed. The mineralization process was performed with the use of 65% HNO₃ (Suprapur) and 70% HClO₄ (Suprapur) according to the procedure proposed by Massaquoi et al. (2015). First, homogenized plant material (0.5 g of subsample−0.001 g accuracy) was mineralized at 60 °C for 12 h. After that, nitric acid was used for evaporation at 130 °C. When the samples cooled down, 70% HClO₄ (Suprapur) was added to each sample, and the samples were heated to 220 °C. The mineralized subsamples were diluted with 10 mL of 0.1 M HNO₃

Table 1

Average heavy metal concentrations ($\pm$SD) in mg/kg d.w. in organs of *P. australis* seedlings collected from uncontaminated (S_{uncont}) and contaminated (S_{cont}) sites (Nawrot et al., 2019).

Site	Plant part	Heavy metal concentrations [mg/kg d.w.] in plant tissues																				
		Cu			Zn			Pb			Cd			Ni			Cr		
S_{uncont}	BG	3.19	$\pm$	0.11	23.1	$\pm$	1.1	2.88	$\pm$	0.16	0.107	$\pm$	0.005	1.69	$\pm$	0.07	3.81	$\pm$	0.16
	ST	0.827	$\pm$	0.029	11.7	$\pm$	0.5	0.153	$\pm$	0.01	0.007	$\pm$	0	0.264	$\pm$	0.012	0.241	$\pm$	0.010
	LF	1.92	$\pm$	0.07	24.5	$\pm$	1.1	0.212	$\pm$	0.012	0.015	$\pm$	0	0.845	$\pm$	0.037	0.219	$\pm$	0.009
S_{cont}	BG	66.2	$\pm$	2.3	691	$\pm$	32	4.43	$\pm$	0.24	0.833	$\pm$	0.038	12.4	$\pm$	0.55	6.84	$\pm$	0.29
	ST	14.4	$\pm$	0.5	473	$\pm$	22	0.109	$\pm$	0	0.055	$\pm$	0.003	0.594	$\pm$	0.026	0.901	$\pm$	0.038
	LF	11.3	$\pm$	0.4	340	$\pm$	16	0.039	$\pm$	0	0.021	$\pm$	0	1.06	$\pm$	0.05	0.868	$\pm$	0.037

BG – belowground organs: roots and rhizomes; ST – stems; LF - leaves.

(Suprapur) and placed in PP test tubes. Plant samples were analyzed using inductively coupled plasma mass spectrometry (ICP-MS) (Perkin Elmer). All analyses were performed in three replicates, and the results for *P. australis* were given on a dry weight basis. Blank samples were measured according to the same procedure. Analytical accuracy was determined using a certified reference of strawberry leaves (LGC716). Recoveries were within 10% of the certified values.

2.2.2. Sediments

Sediment samples for chemical analyses were collected before the experiment started (as described in 2.1.). At the end of the experiment, sediment samples were taken from the 0–10 cm layer of the test sediments and from depths near the plant roots. Then, samples were mixed, homogenized, and transported to the laboratory. Next, sediments for trace metal analyses were lyophilized to a constant weight and homogenized again. Mineralization was performed with the use of $HClO_4$, HF, and HCl (3:2:1; Suprapur) according to the procedure described by Vallius and Leivuori (1999) and Zaborska (2014). Sediment samples were analyzed using ICP-MS Perkin Elmer. All analyses were performed in three replicates, and the results for the analyzed sediments were given on a dry weight basis. Blank samples were measured according to the same procedure. Analytical accuracy was determined using certified reference sediments (IAEA-433). Recoveries in the range of 93–103%, depending on individual metals, were achieved, thus indicating good agreement between standard and analytical values.

The precision, given as the relative standard deviation, was in the range of 3–5%. The limits of detection (LODs) of each element were set at $3 \cdot SD$ (blank), where the SD values were the standard deviations of the blank samples ($n = 5$). LODs were as follows: Zn = 0.5 mg/kg d.w., Cu = 0.3 mg/kg d.w., Pb = 1.0 mg/kg d.w., Cr = 1.5 mg/kg d.w., Ni = 0.7 mg/kg d.w., Cd = 0.1 mg/kg d.w. The limit of quantification (LOQ) for a given element was set at $9 \cdot SD$ (blank), and ranged from 0.2 mg/kg (Cd) to 0.9 mg/kg (Pb). The LOQ is usually established as the difference between two distinct concentrations that could be measured.

The sediment pH was determined with a pH meter (Extech Instrument) by inputting the probe into the analyzed sediments. The pH was checked over the entire experimental period. The total organic matter content in the sediments was determined by combustion of dried sediments at 450 °C for 2 h in a muffle furnace (Carbolite); it was assumed that the loss during heating corresponded to the proportion of organic substances in the analyzed samples.

2.3. Microscopy procedures

Two times during the investigation period, freshly cut plant tissues of C3 S_{uncont} and CONTROL *P. australis* seedlings were placed in PE bags and immediately transported to the laboratory for SEM analysis with a QUANTA FEG 250. The CONTROL samples were collected in April 2018 and grown in sediments from the original site stored in a tank filled with tap water during the entire experimental period. In the laboratory, the tissue preparations (dimensions in the projection - 0.5 cm^2) were placed on a flat mat with a supporting surface of approximately 1 cm^2, placed in the handle, and inserted into the chamber. Nonconductive

samples were sprayed with a thin layer of gold (Au (99.99%) - 10 nm) with a LEICA EM SCD 500 vacuum sprayer. This layer plays the roles of conducting electric current and protecting the test material against damage from the electron beam (Pathan et al., 2009). The observation was performed in a low vacuum (LV-SEM - Low Vacuum Scanning Electron Microscopy). The basic parameters of the SEM were as follows: vacuum pressure of approx. 70 Pa, HV = 5 kV, detection via large field detector (LFD), secondary electron (SE) mode, magnification from 10× to 100,000×, and working distance (WD) of approx. 10 mm.

2.4. Metal uptake efficiency assessment

To quantify the phytoextraction efficiency, the bioconcentration factor (BF) (Ali et al., 2013) and translocation factor (TF) (Bonanno and Vymazal, 2017) were used. The BF shows the plants' ability to accumulate a metal into their tissues from the surrounding environment (sediments). The BF is expressed by the following Formula (1):

$$BF = \frac{trace\ element_{BG}}{trace\ element_{sediments}} \tag{1}$$

The TF shows the efficiency of the plant in translocating the accumulated metal from its belowground (BG) parts (roots and rhizomes) to stems (ST) and leaves (LF) and between aboveground (ABG) parts (ST and LF), according to Formulas (2), (3), and (4), respectively:

$$TF_{ST/BG} = \frac{trace\ element_{ST}}{trace\ element_{BG}} \tag{2}$$

$$TF_{LF/BG} = \frac{trace\ element_{LF}}{trace\ element_{BG}} \tag{3}$$

$$TF_{LF/ST} = \frac{trace\ element_{LF}}{trace\ element_{ST}} \tag{4}$$

The concentration in roots and rhizomes (BG parts) was determined for these parts together. The concentration in ST and LF (ABG parts) was evaluated using Formula (5) (Vymazal, 2016):

$$ABG = \frac{trace\ element_{ST} \cdot weight_{ST} + trace\ element_{LF} \cdot weight_{LF}}{weight_{ST} + weight_{LF}} \tag{5}$$

To determine the accumulation [μg/m^2] of metals in plants, the concentrations [mg/kg = μg/g = ppm] in ABG and BG parts were calculated in terms of the biomass weight [g] per m^2.

Plant height and the external appearance of plants were measured and observed to detect possible senescence. The relative growth rate (RGR) (% · day^{-1}) was calculated in each column considering the initial and final plant heights, according to Eq. (6) as described by Gao et al. (2018):

$$RGR = 100 \frac{\ln(H_2/H_1)}{T_2 - T_1} \left[\frac{\%}{day}\right] \tag{6}$$

where H_1 and H_2 are the initial and final plant heights (cm), respectively, and $(T_2 - T_1)$ is the experimental period (days).

The chemical analysis results correspond to the mean of three replicates. All values are reported as the mean and the standard deviation (SD) of the mean unless otherwise noted.

2.5. Sediment contamination status

To assess the contamination status of the dredged sediments used in the mesocosm setup, the German Länder-Arbeitsgemeinschaft Wasser classification (LAWA) (LAWA-Arbeitskreis, 1998) and pollution load index (PLI) were used (Tomlinson et al., 1980). The PLI was calculated according to Formula (7):

$$PLI = \sqrt[n]{CF_1 \cdot CF_2 \cdot \ldots \cdot CF_n} \qquad (7)$$

where CF is the contamination factor calculated for each metal separately according to Eq. (8):

$$CF = \frac{Cm_{Sample}}{Cm_{Backgroud}} \qquad (8)$$

where Cm_{Sample} is the trace metal concentration in the analyzed sample and $Cm_{Background}$ is the geochemical background concentration of the trace metal. The $Cm_{Background}$ value was established in accordance with Nawrot et al. (2020b). A PLI value <1 corresponds to excellent sediment quality, PLI = 1 shows that only baseline levels of pollutants are present, and PLI > 1 indicates deterioration of site quality.

3. Results & discussion

3.1. Trace metal contents in sediments and plants

3.1.1. Sediment contamination status of dredged sediments applied to mesocosms

Data on the trace metal contents in the dredged sediments used in the mesocosm setup are presented in Table 2. The sediments presented

diverse contamination statuses from moderately contaminated in C2 to very strongly contaminated in C1, according to LAWA-Arbeitskreis (1998). The PLI identified the deterioration of quality in the sediments collected from retention ponds in the Strzyza stream area (C1 and C3). The pH values of the sediments used the columns varied from 7.1–7.4 during the experimental period. The organic matter content was 7.5% in C1, 13.5% in C2, and 11.5% in C3.

3.1.2. Trace metal concentrations in P. australis tissues tested in the mesocosms

Trace metal concentrations in P. australis tissues at the middle and end of the investigation period in relation to the initial PTE contents for S_{uncont} and S_{cont} seedlings are presented in Fig. 2a–b. The average ± SD values are presented in Table S.2. In general, the concentrations of all studied trace metals were significantly higher in BG than in ABG biomass. The trace metal contents in S_{uncont} and S_{cont} decreased in the following order: Zn > Cu > Pb > Cr > Ni > Cd.
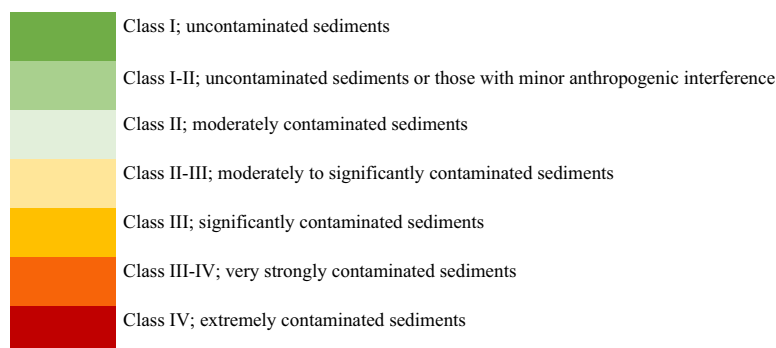
With regard to S_{uncont}, the overall trace metal concentrations in BG parts, ST, and LF presented an increase during the 6 months of the experiment. The highest Cu, Cd, and Ni concentrations in S_{uncont} for the BG parts occurred in C2, with 15.4, 0.25, and 6.99 mg/kg d.w., respectively, while those for Zn were observed in C3 at 155 mg/kg d.w., and those for Pb and Cr were observed for C1 at 39.2 and 9.87 mg/kg d.w., respectively. Metal concentrations increased on average in the BG parts from 1.2 times for Cd to 5.7 times for Pb from the baseline levels, in LF from 1.5 times for Pb to 6.0 times for Zn, and in ST from 1.1 times for Pb to 2.3 times for Zn. The highest increase in Cu inside the BG and ABG tissues occurred in C3; the intense Cu accumulation in the whole P. australis body could be related to the sufficient (at the level of 130 mg/kg d.w.) Cu availability in the sediments (soil). Pb and Ni were mainly accumulated by the BG parts, while Cd and Cr increases were observed in both BG parts and ST. From the middle of the research period to the end of the experiment (VI - IX 2018), the increase in trace metals throughout P. australis tissues was in the range of 1 to 2 times. A sharp increase in concentration was noted only in the cases of Zn in C2 LF (11 times) and C3 LF (3.4 times), Pb in C3 BG parts (2.8 times); and Ni in C1 ST (2.4 times).

Table 2
The average trace metal concentration [mg/kg d.w.] ± SD in dredged sediments placed in the mesocosm setup and the assessment of sediment contamination with the use of LAWA classification (LAWA-Arbeitskreis, 1998) and the pollution load index (PLI) (Tomlinson et al., 1980).

Column	Sediment origin	Average trace metal concentrations [mg/kg d.w.] in dredged sediments						PLI
		Cu	Zn	Pb	Cd	Ni	Cr	
C1$_{u,c}$	Ogrodowa	23.9 ± 1.2	803 ± 9	667 ± 4	0.308 ± 0.004	10.8 ± 0.8	27.7 ± 1.1	6
C2$_{u,c}$	Grunwaldzka	36.5 ± 2.1	189 ± 2	97.9 ± 1.2	0.301 ± 0.011	6.92 ± 0.9	24.9 ± 0.8	1
C3$_{u,c}$	Potokowa	128 ± 3	629 ± 8	98.9 ± 2.4	0.552 ± 0.009	23.4 ± 1.1	60.4 ± 1.5	8

Explanation:

Class I; uncontaminated sediments

Class I-II; uncontaminated sediments or those with minor anthropogenic interference

Class II; moderately contaminated sediments

Class II-III; moderately to significantly contaminated sediments

Class III; significantly contaminated sediments

Class III-IV; very strongly contaminated sediments
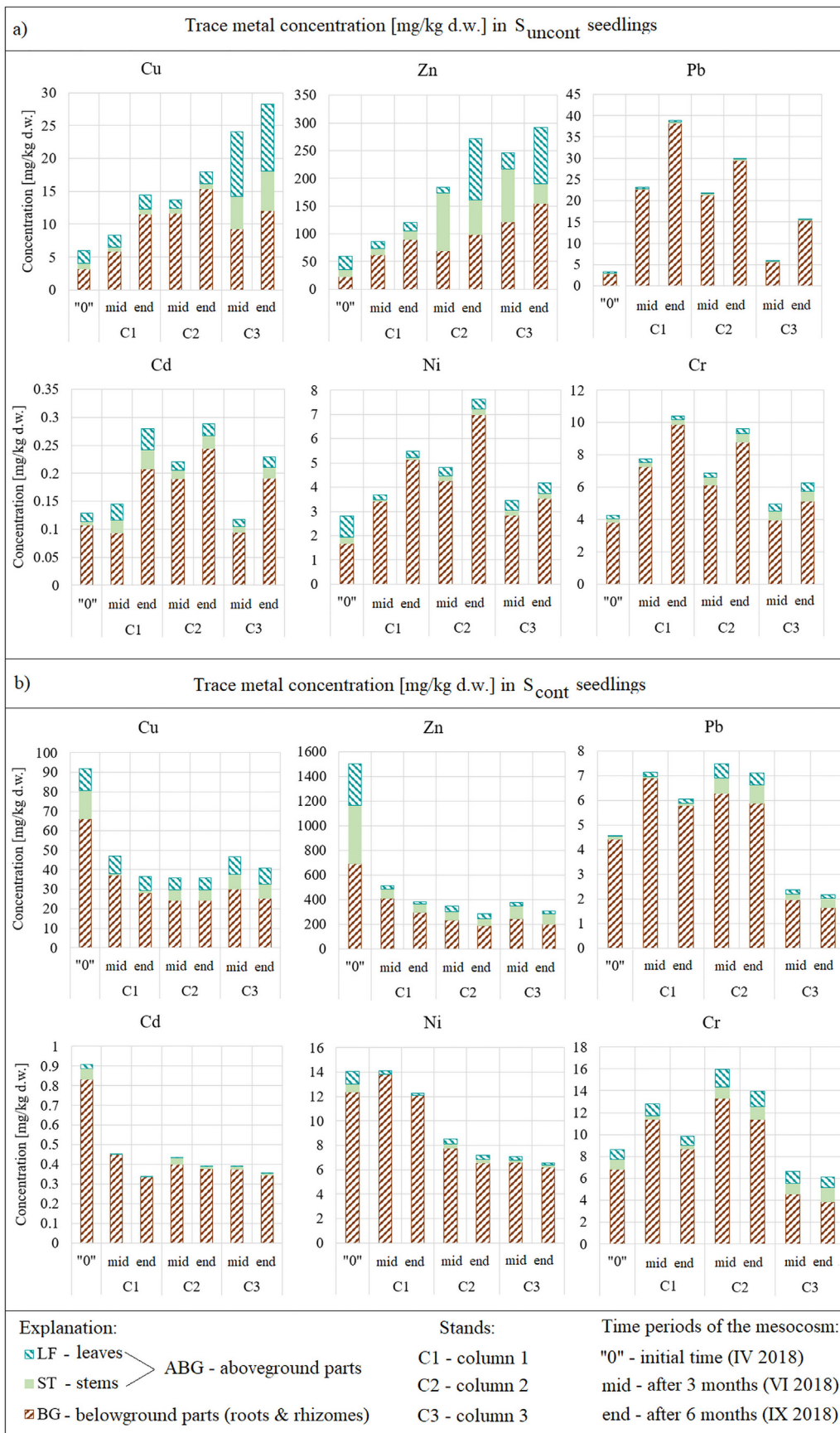
Class IV; extremely contaminated sediments

Fig. 2. Average trace metal contents in *P. australis* seedlings: S_{uncont} and S_{cont} at the middle (mid) and end of the investigation period [mg/kg d.w.] in relation to the initial trace metal contents.

The S_{cont} seedlings of *P. australis* showed a general tendency of decreased metal contents inside their tissues. During the first 3 months, seedlings took up only Pb and Cr; the concentrations of other PTEs showed a decreasing trend. The average increase in Pb in the BG parts was from 1.4 (C2) to 1.6 (C1) times, while that in ST was from 0.5 (C1) to 6.0 (C2) times, and that in LF was from 4.5 (C1) to 14.3 (C2) times. In the case of Cr, the increase was definitely lower – from 1.2 (in C2 ST) to 1.9 times (in C2 BG). Between VI and IX 2018, *P. australis* continued to show decreasing metal contents; only in the case of ST (C1 and C3) was the increase in Pb of 1.5 times noted. The initial concentration of analyzed PTEs inside S_{cont} was much higher than that inside S_{uncont}. This can explain the insufficient ability of S_{cont} plants to accumulate additional trace elements from dredged sediments.

3.1.3. Trace metal accumulation in P. australis

Trace metal accumulation $[\mu g/m^2]$ in ABG and BG parts of *P. australis* at the end of the investigation period in comparison to the initial trace metal content inside the seedlings is presented in Fig. 3. The biomass $[gDM/m^2]$ of harvested *P. australis* from each column of the mesocosm is presented in Table S.1. The pH values of the source sites of S_{uncont} and S_{cont} were in the ranges of 6.9–7.2 and 6.3–6.9, respectively. Plant growth and biomass increases are directly related to soil/sediment pH; pH determines the availability of nutrients to plants and metal toxicity in plants (Corzo Remigio et al., 2020).

High biomass for S_{uncont} was observed in C2 (in gDM/m^2 for ABG - 38.24 and BG - 24.95); this was 2 times higher in relation to the ABG biomass of C1 and C3, while in relation to the BG biomass of C3 and C1, it was 1.6 and 4.3 times higher, respectively. As a result, the accumulation (in $\mu g/m^2$) was the highest for C2 BG and was (in $\mu g/m^2$) as follows: Cu – 768, Zn – 4915, Pb – 1467, Cd – 12.2, Ni – 349, and Cr – 439. High accumulation of Zn was also observed in C2 ABG at 6742 $\mu g/m^2$ and C3 BG at 4855 $\mu g/m^2$. Despite the highest concentration of Cr in C1, the accumulation per 1 m^2 was not high due to the lower biomass development; the accumulation was 4 times lower than the highest accumulation of Cr observed for S_{uncont} C2. The Cr content in dredged sediments (especially in C1 and C3) could affect proper *P. australis* development. According to Shanker et al. (2005), the toxic effect of Cr on plants is visible, manifesting as poor plant growth, alterations in the germination process and in the growth of roots, stems, and leaves, and plant physiological processes.

For S_{cont}, the highest concentrations of PTEs in the BG parts were observed for Cu, Zn, and Ni in C1 – 28.2, 295, and 12.1 mg/kg d.w., respectively, and for Pb, Cd, and Cr in C2 – 5.87, 0.38, and 11.4 mg/kg d.w., respectively. The highest biomass of S_{cont} was noted for C2 (in gDM/m^2 for ABG - 34.80 and BG – 29.48); the ABG biomass of C2 was 2 times higher than that of C1 and 2.5 times higher than that of C3, while the C2 BG biomass was 2.5 higher than that of C3 and almost 4 times higher than the C1 biomass. Therefore, accumulation was highest for C2 for all analyzed PTEs and was (in $\mu g/m^2$) as follows: Cu – 1114, Zn – 11,026, Pb – 346, Cd – 22.3, Ni – 388, and Cr – 672. In general, the accumulation of PTEs was higher for S_{cont} than S_{uncont}; only in the case of Pb was an inverse relationship observed.

3.2. Phytoextraction efficiency of P. australis

The BF, as an indicator of metal accumulation efficiency, is presented in Fig. 4. When the BF is greater than 1, the plant shows potential for efficient phytoextraction. At the middle of the experiment (VI 2018), the BF values for S_{uncont} *P. australis* were all below 0.7, while at the end of the experiment, they increased, reaching the highest level > 1 for Ni in C2. In the case of S_{cont}, the opposite trend was trend. At the middle of the experiment, BF values greater than 1 were observed for Ni and Cd in C1 and C2 as well as for Cu (only C1) and Zn (only C2). No BF

exceeding 1 was noted in C3. At the end of the experiment, a decrease in BF values for all metals for S_{cont} samples was observed, showing an adverse trend for phytoextraction.

The BF values reported by Bonanno and Vymazal (2017) for *P. australis* were as follows: 0.32 for Cu, 1.42 for Zn, 0.23 for Pb, 3.77 for Cd, 0.46 for Ni, and 0.31 for Cr. In this study, similar results were obtained for Pb and Cr, for which the BF values ranged from 0.1–0.3 and 0.1–0.5, respectively. The increasing BF values observed during the 6 months of the experiment for S_{uncont} indicate that common reed is a PTE-tolerant species. The sediments applied to C3 presented a similar analyzed PTE content at the source sites of S_{cont} seedlings (Nawrot et al., 2019); therefore, easy adaptation and efficient phytoextraction of *P. australis* seedlings originating from that site was expected. However, these expected behaviors could be disturbed by the pH and organic matter content differences between the source site and tested sediments (note that the pH in the source site for S_{cont} was 6.9–7.4; the pH values of dredged sediments applied in the mesocosm setup were in the ranges 7.1–7.4, while the organic matter content was on average 10.8%). Despite the wide pH tolerance (between 2.5 and 9.8 for the most extreme conditions) of *P. australis* (Packer et al., 2017), Shaltout et al. (2006) emphasized that "the clones growing at a particular site are probably well adapted to those site conditions and possibly do not thrive in other conditions". Thus, the choice of proper *P. australis* seedling clones is quite important in planning the treatment processes of contaminated sites. The BF values for S_{cont} decreased during the experiment, which could be explained by the plant response to PTE contamination of sediments and by the high initial enrichment of S_{cont}. It can be stated that during the single cycle of *P. australis* vegetation, S_{uncont} seedlings were able to uptake PTEs and could be used for phytoimmobilization purposes. At the same time, for the optimal performance of the phytoextraction process, there is a need to carry out phytoremediation tests for at least 2 or more growing seasons (Kumari and Tripathi, 2015). Moreover, the organic matter content, the right amount of light (our experiment took place under semiartificial conditions), and proper pH are conditioning factors for good growth and development of common reed, along with its full phytoextraction efficiency (Shaltout et al., 2006). pH is considered the most important single factor that influences the availability of PTEs from solid materials (Antoniadis et al., 2017b). The lower the pH is for cationic species (e.g., Zn^{2+}, Ni^{2+}, Cr^{3+}, Pb^{2+}, Cu^{2+}, Cd^{2+}), the higher the mobility and availability, while the opposite relationship holds true for anionic species. Metallic PTE sorption increases with increasing sediment/soil pH. Moreover, during the basic process of increasing the pH of acidic soils – liming – decelerating metal mobility and decreasing cationic PTE availability is noted. Therefore, this results in increasing metal availability for plants attributed to the precipitation of soluble metals in the carbonate fraction, which are considered easily mobilized in the acidic rhizosphere zone (Antoniadis et al., 2017a).

The TF values between different pairs of *P. australis* tissues are presented in Table 3. Considering metal translocation between the BG parts and ST, the TF for both S_{uncont} and S_{cont} indicates low translocation. The highest values were observed for Zn in the S_{uncont} seedlings of C2 and C3 ($TF_{ST/BG}$ = 0.6 at both sites). Other TF values were low, between 0.0 and 0.5, indicating no or little translocation of metals between roots and stems. The translocation between LF and BG parts was observed in S_{uncont} for Cu (C3; $TF_{LF/BG}$ = 0.8) and Zn (C2 and C3; $TF_{LF/BG}$ = 1.1 and 0.7, respectively). $TF_{LF/ST}$ was definitely higher than the translocation between BG organs and either ST or LF for both S_{uncont} and S_{cont}. A $TF_{LF/ST}$ > 1 was observed in several cases for all analyzed trace elements. The TF values between the BG and ABG organs of *P. australis* indicate that the PTEs taken up from the sediments were stored in roots and rhizomes and not translocated to the ABG parts responsible for vital photosynthetic processes. This could be partly due to low accumulation or to
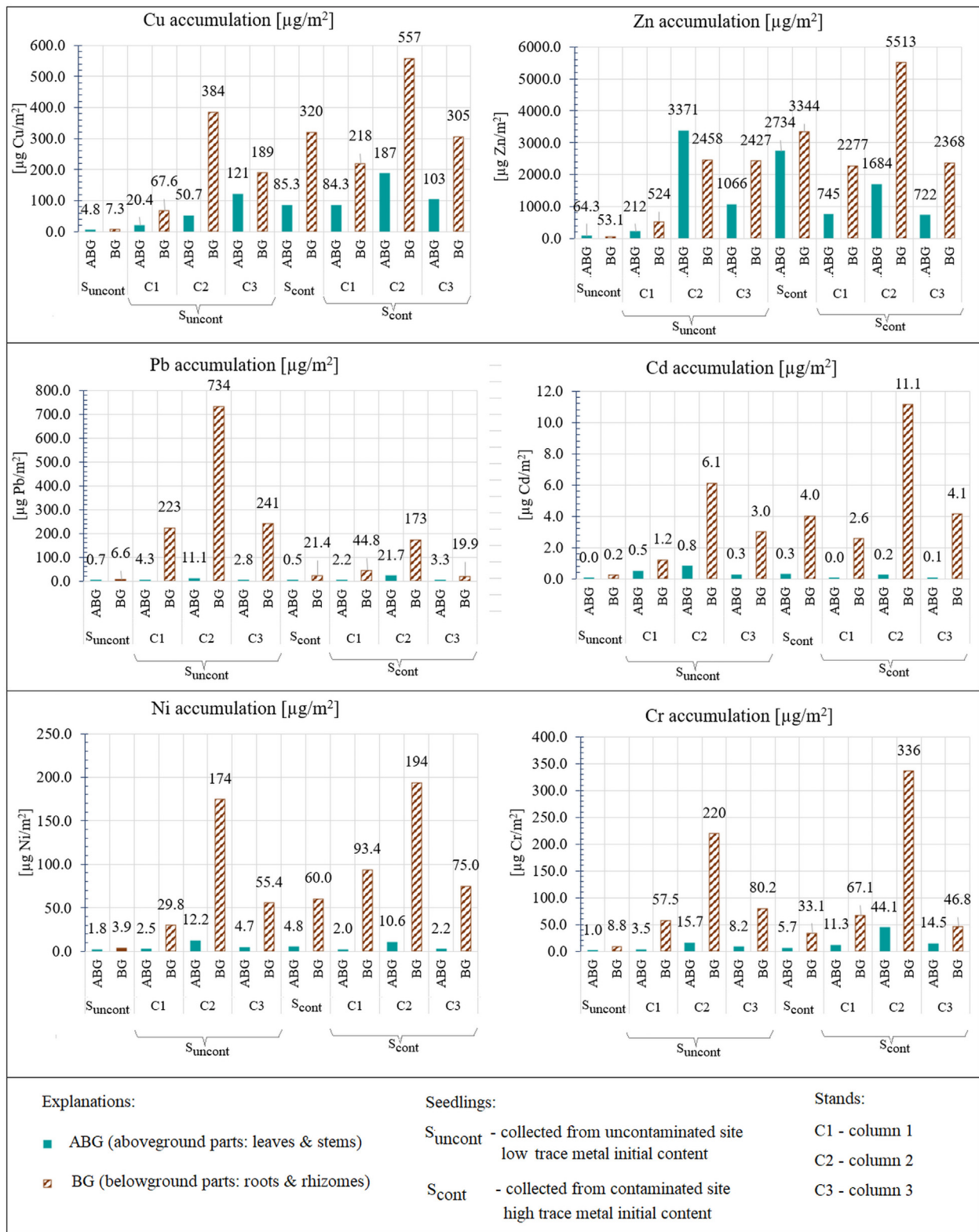
Fig. 3. Trace metal accumulation [µg/m²] in aboveground (ABG) and belowground (BG) parts of *P. australis* S$_{uncont}$ and S$_{cont}$ samples at the end of the investigation period. Please note the different scales.

effective protective mechanisms against metal translocation to the most essential plant organs. Only Zn and Cu were to some extent transmitted to the ABG parts, reflecting either the plants' demand for these microelements or their lack of toxicity. The TF$_{ST/BG}$ in S$_{uncont}$ and S$_{cont}$ indicated that in the 1st stage of growth on contaminated sediments in the mesocosm, *P. australis* was a tolerant species (according to Ashraf et al., 2011) to PTE occurrence, and translocation mainly occurred between ST and LF.
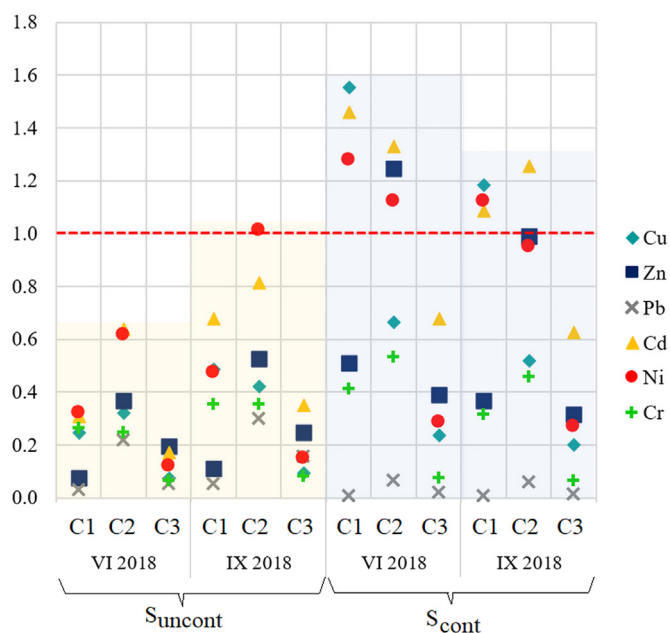
8

Fig. 4. The bioconcentration factor (BF) for S$_{uncont}$ and S$_{cont}$ *P. australis* at the middle (VI 2018) and end (IX 2018) of the investigation period; S$_{uncont}$- seedlings collected from the uncontaminated site and S$_{cont}$ – seedlings collected from the contaminated site, C1, C2, C3- columns 1, 2, and 3, respectively.

3.3. Comparison of S$_{ucont}$ and S$_{cont}$ performance

S$_{uncont}$ as "clean" clones of the mother plants presented phytostabilization abilities. According to Sarwar et al. (2017), most of the 5 major steps of the phytoextraction mechanism were achieved by S$_{uncont}$: metal mobilization in the rhizosphere, metal ion uptake by plant roots, translocation to aerial plant parts, metal sequestration in plant tissues, and metal tolerance. The results of this study confirm the low movement of Pb to the ABG parts of *P. australis*, which is in

Table 3
The translocation factors (TFs) for S$_{uncont}$ and S$_{cont}$ *P. australis* at the end (IX 2018) of the investigation period; S$_{uncont}$- seedlings collected from an uncontaminated site and S$_{cont}$ – seedlings collected from a contaminated site, C1, C2, C3- column 1,2, and 3, respectively.

Site	Translocation Factor					
	Cu	Zn	Pb	Cd	Ni	Cr
ST/BG						
C1 S$_{uncont}$	0.1	0.2	0.0	0.2	0.0	0.0
C2 S$_{uncont}$	0.0	**0.6**	0.0	0.1	0.0	0.1
C3 S$_{uncont}$	0.0	**0.6**	0.0	0.1	0.0	0.1
C1 S$_{cont}$	0.0	0.2	0.0	0.0	0.0	0.0
C2 S$_{cont}$	0.3	0.3	0.1	0.0	0.0	0.1
C3 S$_{cont}$	0.3	0.5	0.2	0.0	0.0	0.3
LF/BG						
C1 S$_{uncont}$	0.2	0.2	0.0	0.2	0.0	0.0
C2 S$_{uncont}$	0.1	**1.1**	0.0	0.1	0.1	0.0
C3 S$_{uncont}$	**0.8**	**0.7**	0.0	0.1	0.1	0.1
C1 S$_{cont}$	0.3	0.1	0.0	0.0	0.0	0.1
C2 S$_{cont}$	0.3	0.2	0.1	0.0	0.1	0.1
C3 S$_{cont}$	0.3	0.1	0.1	0.0	0.0	0.3
LF/ST						
C1 S$_{uncont}$	**3.0**	**1.0**	**1.0**	**1.1**	**2.1**	0.6
C2 S$_{uncont}$	**2.6**	**1.8**	0.9	**1.0**	**1.6**	0.6
C3 S$_{uncont}$	**0.8**	**0.7**	0.0	0.1	0.1	0.1
C1 S$_{cont}$	**7.5**	0.3	**2.0**	**2.0**	**23.4**	**3.1**
C2 S$_{cont}$	**1.2**	**0.7**	**0.6**	0.3	**1.3**	**1.3**
C3 S$_{cont}$	**1.2**	0.3	**0.5**	0.3	**1.8**	**0.8**

Bold emphasis statistically significance at TF ≥ 0.5.

line with the generally known Pb behavior in soil/sediments (Thakur et al., 2016). Enrichment of the Pb content in roots is considered to be due to epidermal exclusion (MacFarlane et al., 2003). The highest increase in Cu concentration in ABG and BG parts was noted in highly contaminated sediments (C3–128 mg/kg d.w.), while in other columns, the increase in Cu occurred only in the BG parts. In general, a concentration of 2 mg/kg d.w. of Cu is sufficient to meet the physiological demands of plants. In addition, plants are relatively resistant to Cu toxicity (Yadav, 2010). Cu and Zn interactions are recognized as antagonistic for plants (Kabata-Pendias and Pendias, 1999); however, Singh et al. (2016) reported that the amount of Cu in BG parts increased in the presence of Pb and/or Zn. For S$_{uncont}$ in C1 (where the maximum Zn contamination occurred), the increase in Cu and Zn was the lowest: 1.7 times for Cu and 2.7 times for Zn (the Zn:Cu ratio in sediments was 33). In C3, where the increase in these PTEs was the highest (3 times for Cu and 5.2 times for Zn), the ratio of Zn:Cu was approx. 5. Zn was translocated to ABG parts to a higher extent than other metals; however, Cd demonstrated an increase in ST. Zn concentrations of up to 630 mg/kg d.w. did not interfere with the uptake of this metal by LF and ST, however, this process was disturbed at a concentration of approx. 800 mg/kg (C1 S$_{uncont}$). Due to the presence of the growth hormone indole acetic acid, Zn can exhibit higher concentrations in stems than in other plants parts (Minkina et al., 2018). The synergistic reactions of Cd and Zn in plants are adjacent to the root system (Kabata-Pendias and Pendias, 1999). A substantial increase in Cd concentration was observed at the end of the experiment. The most apparent symptom of Cd toxicity is the retardation of plant growth (Xie et al., 2014). However, Ederli et al. (2004) did not identify visual symptoms of Cd toxicity in *P. australis*; moreover, their experiment proved the suitability of this species for Cd detoxification. Ni shows affinity (antagonistic and/or synergistic) to Cu, Zn, and Cd (Kabata-Pendias and Pendias, 1999). In the middle of the investigation period, the Ni content increased similarly to that of Cd during all 6 months (similar properties in Ni and Cd uptake).

S$_{cont}$, as trace metal-enriched clones of the mother plant, did not perform phytoextraction and moreover showed an adverse effect of metal release referred to as phytoexclusion. Metal transport occurs in the xylem and is largely due to transpiration (Rucińska-Sobkowiak, 2016). PTEs can be actively or passively intercepted; the first pathway requires metabolic energy (Thakur et al., 2016), while the second occurs by diffusion. Metals are mostly bound with BG parts, and 95% or more of the absorbed elements are sequestered in the plant roots unless the plant is a hyperaccumulator or are chelate-assisted (Shahid et al., 2015). The movement of metal ions can be accomplished by restricting metal transport across the root endodermis (stele), storage in cell walls and vacuoles, or binding by metal-binding proteins (Weis et al., 2004). Otherwise, these ions are transported via the water flow of the vascular system to ABG parts. Shahid et al. (2015) emphasized that in addition to the absorption of PTEs by BG parts, exudation could occur (phytoexclusion).

The accumulation of PTEs by S$_{uncont}$ and S$_{cont}$ was lower than that reported by Vymazal and Březinová (2016). In a horizontal flow constructed wetland for wastewater treatment, the following metal concentrations were noted for *P. australis* (in µg/m^2): 2130–9190 for Cu, 1220–9500 for Zn, 6–620 for Pb, 38–2640 for Cd, 460–8800 for Ni, and 570–7740 for Cr (Vymazal and Březinová, 2016). Reed is obviously not among the most sensitive species to metals; however, its metal accumulation strongly depends on plant uptake capacity and transport inside the whole plant and at the cellular level (Gupta et al., 2016). Despite the capture of metals by S$_{uncont}$ and loss by S$_{cont}$, the highest accumulation of Cu, Zn, Cd, Ni, and Cr occurred for S$_{cont}$, while that of Pb occurred for S$_{uncont}$. It is worth highlighting and recalling here that in the area of 0.5 m^2, only 3–4 seedlings were planted. This fact, together with the growth response of *P. australis*, explains the low values of accumulation obtained under the experiment. This study showed that there are different patterns of metal concentration and accumulation. The

general conclusion to be drawn from our results is that accumulation efficiency is generally biomass-size independent. A greater biomass may result in a higher quantitative bioaccumulation capacity (higher total concentration); however, a higher qualitative bioaccumulation capacity means more efficient accumulation (Bonanno and Vymazal, 2017). Roots are primary sites for PTE accumulation, and further PTE movement as a response to plant stress may be restricted (Minkina et al., 2018; Vymazal, 2016).

3.4. Anatomical and morphological responses of P. australis

3.4.1. Relative growth rate

The *P. australis* relative growth rate (RGR) is presented in Table S.3. During the first 75 days, the growth of the seedlings ranged from 60 to 80 cm. The RGR changed from 1.6 to 2.2%·day^{-1}. Engloner (2009) reports that the RGR of shoots is highest from April–May, and growth is faster in potentially taller than shorter shoots. This is in line with the results obtained in this study because the RGR over the next 75 days was lower than the initial RGR (with changes between 0.9 and 1.3%·day^{-1}). In general, *P. australis* growth was the highest for S_{uncont} and S_{cont} in C2 and the lowest in C3. The average growth of *P. australis* per length of aboveground shoots was 20 cm per month.

3.4.2. Microscopic analysis of plant tissues

SEM examination of *P. australis* semifine sections from the control site (CONTROL) and S_{uncont} seedlings from C3 (collected in half of the experiment) showed that reed roots consisted of the stele (S), the internal layer formed by the endodermis (EN), the exterior layer formed by the epidermis (EP), and cortical parenchyma (C) between them. The cortex in CONTROL *P. australis* consisted of 6–7 cellular layers of external parenchyma, including a bilayered exodermis and inner aerenchyma (AE) separated from the S by a well-developed EN (Fig. 5.a,c,e). In the parenchymal layer, the cells were round and arranged in regular radial rows. A comparison of the transverse sections of CONTROL and S_{uncont} *P. australis* (Fig. 5.b, d, f) showed differences in cortex formation (irregular cell formation - external parenchyma in some parts consisting of only 2–3 cellular layers). The CONTROL and S_{uncont} *P. australis* also differed in S formation and vessel element (V) arrangement – in S_{uncont}, there were more (quantitatively) Vs forming the cylindrical S. The EN in CONTROL consisting of closely packed parenchymal cells closely adhered to the axis cylinder, while in S_{uncont} *P. australis*, disturbances in EN were observed (in the right part of the image – Fig. 5.d). In Fig. 5.a, b, the differences in lysigenous AE formation in CONTROL and S_{uncont} *P. australis* are presented. Similar results as presented in Fig. 5.b,d,f and were observed at the end of the experiment (Fig. S.2).

The C in CONTROL *P. australis* consisted of constitutively formed lysigenous AE, which is considered regular formation, while in S_{uncont} *P. australis* the lysogenic AE formation was enhanced and formation of a barrier to radial O_2 loss was induced, resulting in the promotion of longitudinal O_2 diffusion to the root apex. A similar observation in lysogenic AE formation was described for rice growing under submerged and waterlogging conditions (Nishiuchi et al., 2012). The rhizodermis cells in the CONTROL roots of *P. australis* (Fig. 5.g) formed substantial root hairs (RHs). For S_{uncont}, the presence of RHs was not as pronounced; moreover, the RHs collapsed (Fig. 5.h).

3.4.3. Plant stress

P. australis indisputably belongs to the group of macrophytes that tend to adapt a tolerance strategy relying on the BG parts as principal accumulator organs. For example, Bonanno and Lo Giudice (2010) described that *P. australis* roots acted as a kind of filter – the Cu amount in rhizomes was reduced by 70%. This kind of behavior is an effective strategy in protecting rhizomes and shoots from Cu-induced injuries (Chai et al., 2014). In this study, the main indicator of PTE toxicity was related to *P. australis* growth and biomass development. The microscopy analysis showed changes in the *P. australis* samples grown in the control

and tested dredged sediments. After 3 months of the experiment, the S_{uncont} reed roots in comparison with the CONTROL roots showed that the PTEs caused the degradation of the EN, significant deformation of AE, and disruption of the orderly arrangement of EP cells. The decrease in air cavities was also noted by Minkina et al. (2018, 2019). This response of roots contacting metal-supplemented sediments probably allows macrophytes to adapt to unfavorable environmental conditions. Collapse of RHs is often reported to have toxic effects (Bini et al., 2012). An important issue related to RHs is that root exudates affect the availability of PTEs at the plant-sediment border. In a few millimeters of area extending from the RHs, the exudates alter the rhizosphere chemistry, which results in an increase in plant tolerance to PTEs. This phenomenon occurs passively (low molecular weight compounds such as sugars, organic acids, amino acids, fatty acids, flavonoids) or actively, but active secretion is highly responsive to PTE exposure. The tolerance to PTEs by plants is dependent on root exudates and therefore could affect the photosynthetic processes. The principal behavior of PTEs is to decrease root exudates and therefore retard photosynthesis, while alleviation of PTE toxicity enhances photosynthetic performance and increases root exudates (Antoniadis et al., 2017a, 2017b). The deformation of LF and chlorosis have been reported in photosynthetic tissues of S_{uncont}, which are common symptoms of metal-stressed plants (Rout and Das, 2003). In this study, the highest concentration in *P. australis* tissues was noted for Zn. Rout and Das (2003) reported that metal toxicity resulted in an increased metal supply to the ABG parts, leading to the disintegration of cell organelles and the disruption of membranes. Membrane stability is often attributed to Zn. As soon as other PTEs pass through the plasma membrane, they can interact with all metabolic processes in the cytosol (Emamverdian et al., 2015).

3.4.4. Trace metal reduction in dredged sediments at the end of the experiment

The trace metal content in sediments decreased after 6 months of the experiment (Table S.4). The general tendency was the improvement of contamination status in the mesocosm setup in all columns in accordance with LAWA classification and the PLI. The observed changes in trace metal contents in most cases were not very high, which was due to low biomass development. Thus, the uptake/release of PTEs by *P. australis* seedlings did not have a significant effect on the final PTE content in sediment. In some cases, an increase in metal content was noted (e.g., Zn - S_{cont} C2, Ni - S_{cont} C1 and C2), which could be related to the S_{cont} seedling release of metals during the experiment (also related to the root exudates).

3.4.5. Potential implications of the study results

The treatment processes of contaminated sites with the use of plants should be preceded by careful analysis of the place of origin and initial PTE content of those plants. The results of our study show different behaviors of *P. australis* seedlings originating from sites with different background PTE contents. The general principle observed in our study was the uptake of metals by S_{uncont} and loss by S_{cont} during the vegetation period. S_{uncont} presented phytostabilization abilities (confirmed by the BF value and accumulation in BG parts) and could meet the requirements for successful phytoextraction mechanisms if the treatment period was extended. The TF classified the S_{uncont} seedlings as PTE tolerant. On the other hand, the S_{cont} seedlings behaved as phytoexcluders, which was probably caused by the change in the concentration of trace metals and pH in the target sediments. Finally, S_{uncont} seedlings presented the plasticity of *P. australis* to adapt to contaminated sites, while S_{cont} seedlings upheld the hypothesis that clones growing at a particular site are well adapted to those site conditions and do not thrive in other conditions or the PTE content in dredged sediments was too low to facilitate uptake by S_{cont} seedlings.

The findings of this study should be further evaluated under real field conditions, since the limitation of our study was the small scale (pot experiment) and the use of semiartificial light. According to
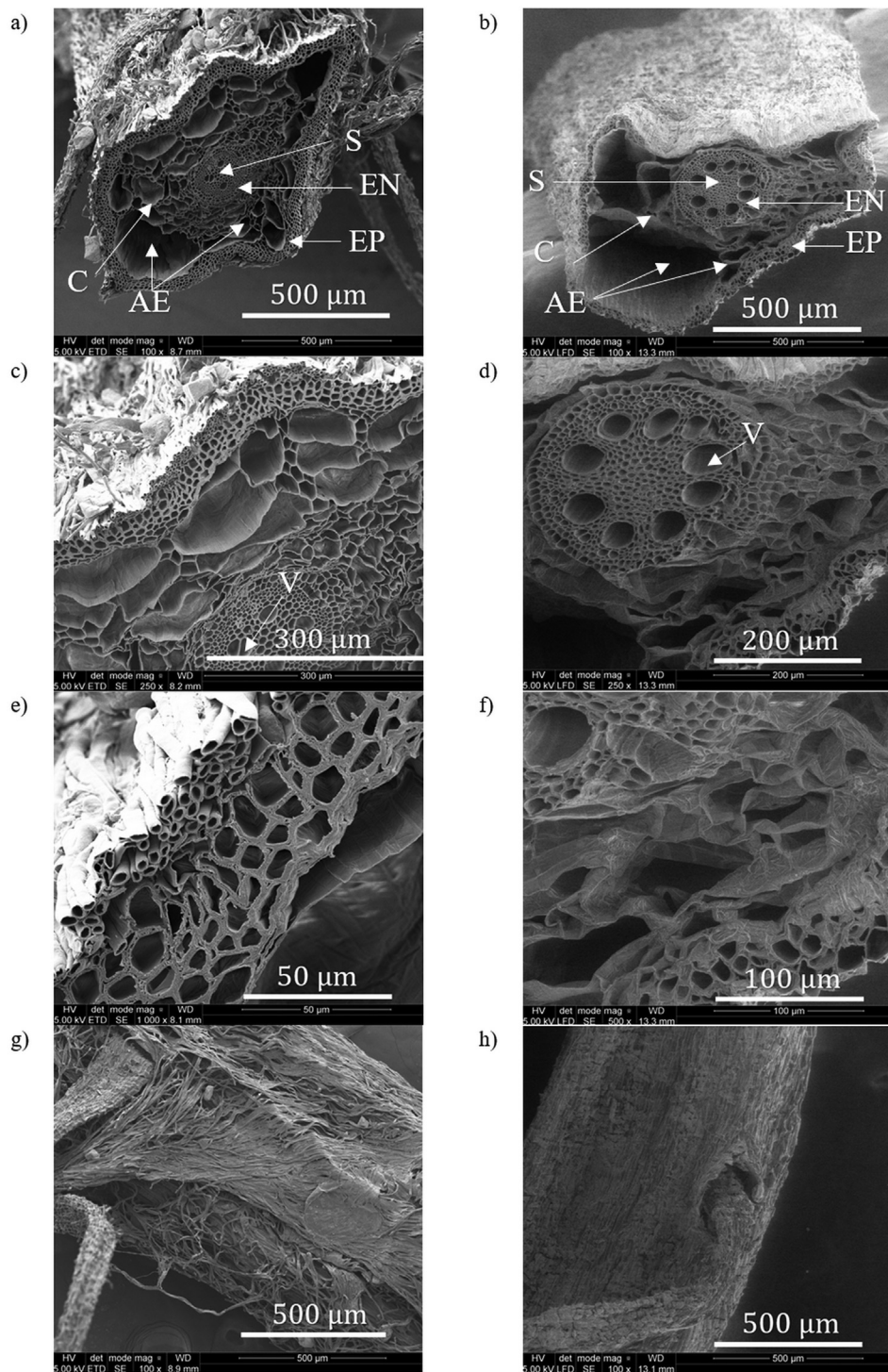

texttext

text

text

text

text

4. Conclusions

P. australis seedlings with different initial trace metal contents (low – S$_{uncont}$ and high – S$_{cont}$) planted in a mesocosm with dredged sediments enriched with Zn, Cu, Pb, Cd, Ni, and Cr were investigated. Dredged sediments placed in the mesocosm setup presented PLI values in the ranges 1–8, corresponding to moderately to very strongly contaminated conditions according to LAWA classification. In general, the different initial contents of trace metals in S$_{uncont}$ and S$_{cont}$ affected the phytostabilization behavior of the seedlings. S$_{uncont}$ adapted to the pot experimental conditions and presented phytostabilization abilities (confirmed by the BF value and accumulation in BG parts). However, despite PTE uptake, during the half-year mesocosm study, disturbance of the ordered arrangement of cortical cells and significant deformation of AE were observed. The main morphological and structural effects caused by metal toxicity can be summarized as follows: (1) growth limitation, (2) root tissue disturbance, (3) collapse of root hairs or decrease in their numbers, (4) structural alterations of epidermis and endodermis. The toxic response of S$_{cont}$ was connected with trace metal release (phytoexclusion). Trace metal uptake in S$_{uncont}$ occurred mainly in BG, especially for Pb and Ni. The accumulation of PTEs was low due to, in general, poor biomass development. However, the highest biomass development was recorded for the sediments least enriched in trace metals (C2), for which the lowest Cr concentration was observed. High biomass is crucial for successful phytostabilization effects. Overall, a decrease in the trace metal content of the dredged sediment was observed during the experiment. According to LAWA classification and the PLI, the contamination status improved.

The mesocosm study results should be further verified in field experiments with the application of *P. australis* and other "native" plants grown in sediments dredged from urban water bodies contaminated with PTEs. The focus should be placed on hydrophyte acclimation to sediments with a low organic matter content, which could be facilitated, for instance, by the addition of biochar.

Funding

CRediT authorship contribution statement

Nicole Nawrot: Conceptualization, Methodology, Investigation, Data curation, Writing – original draft, Writing – review & editing, Visualization, Funding acquisition. **Ewa Wojciechowska:** Conceptualization, Methodology, Writing – original draft, Writing – review & editing, Supervision. **Ksenia Pazdro:** Resources, Formal analysis, Writing – review & editing. **Jacek Szmagliński:** Formal analysis, Resources. **Janusz Pempkowiak:** Supervision, Formal analysis, Writing – review & editing.

Declaration of competing interest

The authors declare that they have no known competing financial interests or personal relationships that could have appeared to influence the work reported in this paper.

Appendix A. Supplementary data

Supplementary data to this article can be found online at https://doi.org/10.1016/j.scitotenv.2021.144983.

References

Achour, R., Abriak, N.E., Zentar, R., Rivard, P., Gregoire, P., 2014. Valorization of unauthorized sea disposal dredged sediments as a road foundation material. Environ. Technol. (United Kingdom) 35, 1997–2007. https://doi.org/10.1080/09593330.2014.889758.

Al-Homaidan, A.A., Al-Otaibi, T.G., El-Sheikh, M.A., Al-Ghanayem, A.A., Ameen, F., 2020. Accumulation of heavy metals in a macrophyte Phragmites australis: implications to phytoremediation in the Arabian peninsula wadis. Environ. Monit. Assess. 192. https://doi.org/10.1007/s10661-020-8177-6.

Ali, H., Khan, E., Sajad, M.A., 2013. Phytoremediation of heavy metals-concepts and applications. Chemosphere 91, 869–881. https://doi.org/10.1016/j.chemosphere.2013.01.075.

Antoniadis, V., Levizou, E., Shaheen, S.M., Ok, Y.S., Sebastian, A., Baum, C., Prasad, M.N.V., Wenzel, W.W., Rinklebe, J., 2017a. Trace elements in the soil-plant interface: Phytoavailability, translocation, and phytoremediation–a review. Earth-Science Rev. 171, 621–645. https://doi.org/10.1016/j.earscirev.2017.06.005.

Antoniadis, V., Levizou, E., Shaheen, S.M., Sik, Y., Sebastian, A., Baum, C., Prasad, M.N. V, Wenzel, W., Rinklebe, J., 2017b. Trace elements in the soil-plant interface: Phytoavailability, translocation, and phytoremediation–a review. Earth-Science Rev. doi:https://doi.org/10.1016/j.earscirev.2017.06.005.

Antoniadis, V., Shaheen, S.M., Stärk, H.J., Wennrich, R., Levizou, E., Merbach, I., Rinklebe, J., 2021. Phytoremediation potential of twelve wild plant species for toxic elements in a contaminated soil. Environ. Int. 146. https://doi.org/10.1016/j.envint.2020.106233.

Ashraf, M.A., Maah, M.J., Yusoff, I., 2011. Heavy metals accumulation in plants growing in ex tin mining catchment. Int. J. Environ. Sci. Technol. 8, 401–416. https://doi.org/10.1007/BF03326227.

Bartoli, G., Papa, S., Sagnella, E., Fioretto, A., 2012. Heavy metal content in sediments along the Calore river: relationships with physical-chemical characteristics. J. Environ. Manag. 95, S9–S14. https://doi.org/10.1016/j.jenvman.2011.02.013.

Bednarova, Z., Kuta, J., Kohut, L., Machat, J., Klanova, J., Holoubek, I., Jarkovsky, J., Dusek, L., Hilscherova, K., 2013. Spatial patterns and temporal changes of heavy metal distributions in river sediments in a region with multiple pollution sources. J. J. Soils Sediments 13, 1257–1269. https://doi.org/10.1007/s11368-013-0706-2.

Bini, C., Wahsha, M., Fontana, S., Maleci, L., 2012. Effects of heavy metals on morphological characteristics of Taraxacum officinale web growing on mine soils in NE Italy. J. Geochem. Explor. 123, 101–108. https://doi.org/10.1016/j.gexplo.2012.07.009.

Bonanno, G., Lo Giudice, R., 2010. Heavy metal bioaccumulation by the organs of Phragmites australis (common reed) and their potential use as contamination indicators. Ecol. Indic. 10, 639–645. https://doi.org/10.1016/j.ecolind.2009.11.002.

Bonanno, G., Vymazal, J., 2017. Compartmentalization of potentially hazardous elements in macrophytes: insights into capacity and efficiency of accumulation. J. Geochem. Explor. 181, 22–30. https://doi.org/10.1016/j.gexplo.2017.06.018.

Chai, M., Shi, F., Li, R., Qiu, G., Liu, F., Liu, L., 2014. Growth and physiological responses to copper stress in a halophyte Spartina alterniflora (Poaceae). Acta Physiol. Plant. 36, 745–754. https://doi.org/10.1007/s11738-013-1452-1.

Cicero-Fernández, D., Peña-Fernández, M., Expósito-Camargo, J.A., Antizar-Ladislao, B., 2017. Long-term (two annual cycles) phytoremediation of heavy metal-contaminated estuarine sediments by Phragmites australis. New Biotechnol. 38, 56–64. https://doi.org/10.1016/j.nbt.2016.07.011.

Corzo Remigio, A., Chaney, R.L., Baker, A.J.M., Edraki, M., Erskine, P.D., Echevarria, G., van der Ent, A., 2020. Phytoextraction of high value elements and contaminants from mining and mineral wastes: opportunities and limitations. Plant Soil, 11–37 https://doi.org/10.1007/s11104-020-04487-3.

Ederli, L., Reale, L., Ferranti, F., Pasqualini, S., 2004. Responses induced by high concentration of cadmium in Phragmites australis roots. Physiol. Plant. 121, 66–74. https://doi.org/10.1111/j.0031-9317.2004.00295.x.

Egene, C.E., Van Poucke, R., Ok, Y.S., Meers, E., Tack, F.M.G., 2018. Impact of organic amendments (biochar, compost and peat) on Cd and Zn mobility and solubility in contaminated soil of the Campine region after three years. Sci. Total Environ. 626, 195–202. https://doi.org/10.1016/j.scitotenv.2018.01.054.

Emamverdian, A., Ding, Y., Mokhberdoran, F., Xie, Y., 2015. Heavy metal stress and some mechanisms of plant defense response. Sci. World J. 2015, 7–9. https://doi.org/10.1155/2015/756120.

Engloner, A.I., 2009. Structure, growth dynamics and biomass of reed (Phragmites australis) – a review. 204, 331–346. https://doi.org/10.1016/j.flora.2008.05.001.

Gao, X., Lee, J.R., Park, S.K., Kim, N.G., Choi, H.G., 2018. Detrimental effects of sediment on attachment, survival and growth of the brown alga Sargassum thunbergii in early life stages. (doi:10.1111/pre.12347).

Gupta, N., Ram, H., Kumar, B., 2016. Mechanism of zinc absorption in plants: uptake, transport, translocation and accumulation. Rev. Environ. Sci. Biotechnol. 15, 89–109. https://doi.org/10.1007/s11157-016-9390-1.

Huang, X., Wang, L., Zhu, S., Ho, S.H., Wu, J., Kalita, P.K., Ma, F., 2018. Unraveling the effects of arbuscular mycorrhizal fungus on uptake, translocation, and distribution of cadmium in Phragmites australis (Cav.) Trin. Ex Steud. Ecotoxicol. Environ. Saf. 149, 43–50. https://doi.org/10.1016/j.ecoenv.2017.11.011.

Kabata-Pendias, A., Pendias, H., 1999. Biogeochemistry of trace elements. Trace Elements in Soils and Plants, Fourth edition https://doi.org/10.1201/b10158-25.

Kumari, M., Tripathi, B.D., 2015. Efficiency of Phragmites australis and Typha latifolia for heavy metal removal from wastewater. Ecotoxicol. Environ. Saf. 112, 80–86. https://doi.org/10.1016/j.ecoenv.2014.10.034.

LAWA-Arbeitskreis, L.-A. "Zielvorgaben" in zusammenarbeit mit, 1998. Beurteilung der Wasserbeschaffenheit von Fliessgewaessern in der BRD. Deutschland. 26.

MacFarlane, G.R., Pulkownik, A., Burchett, M.D., 2003. Accumulation and distribution of heavy metals in the grey mangrove, Avicennia marina (Forsk.)Vierh.: biological indication potential. Environ. Pollut. 123, 139–151. https://doi.org/10.1016/S0269-7491(02)00342-1.

Massaquoi, L.D., Ma, H., Liu, X.H., Han, P.Y., Zuo, S.M., Hua, Z.X., Liu, D.W., 2015. Heavy metal accumulation in soils, plants, and hair samples: an assessment of heavy metal exposure risks from the consumption of vegetables grown on soils previously irrigated with wastewater. Environ. Sci. Pollut. Res. 22, 18456–18468. https://doi.org/10.1007/s11356-015-5131-1.

Milke, J., Gałczyńska, M., Wróbel, J., 2020. The importance of biological and ecological properties of Phragmites Australis (Cav.) Trin. Ex Steud., in phytoremendiation of Aquatic ecosystems—the review. Water 12, 1770. https://doi.org/10.3390/w12061770.

Minkina, T., Fedorenko, G., Nevidomskaya, D., Fedorenko, A., Chaplygin, V., Mandzhieva, S., 2018. Morphological and anatomical changes of Phragmites australis Cav. Due to the uptake and accumulation of heavy metals from polluted soils. Sci. Total Environ. 636, 392–401. https://doi.org/10.1016/j.scitotenv.2018.04.306.

Minkina, T., Fedorenko, G., Nevidomskaya, D., Pol'shina, T., Federenko, A., Chaplygin, V., Mandzhieva, S., Sushkova, S., Hassan, T., Hassan, T.M., 2019. Bioindication of soil pollution in the delta of the Don River and the coast of the Taganrog Bay with heavy metals based on anatomical, morphological and biogeochemical studies of macrophyte (Typha australis Schum. & Thonn). Environ. Geochem. Health 3. https://doi.org/10.1007/s10653-019-00379-3.

Murphy, L.U., Cochrane, T.A., O'Sullivan, A., 2015. The influence of different pavement surfaces on atmospheric copper, Lead, zinc, and suspended solids attenuation and wash-off. Water Air Soil Pollut. 226. https://doi.org/10.1007/s11270-015-2487-2.

Nawrot, N., Wojciechowska, E., 2018. Assessment of trace metals leaching during rainfall events from building rooftops with different types of coverage - case study. J. Ecol. Eng. 19. https://doi.org/10.12911/22998993/85410.

Nawrot, N., Wojciechowska, E., Matej-Łukowicz, K., Walkusz-Miotk, J., Pazdro, K., 2019. Heavy metal accumulation and distribution in Phragmites australis seedlings tissues originating from natural and urban catchment. Environ. Sci. Pollut. Res. https://doi.org/10.1007/s11356-019-07343-9 INNOVATIONS.

Nawrot, N., Wojciechowska, E., Rezania, S., Walkusz-Miotk, J., Pazdro, K., 2020a. The effects of urban vehicle traffic on heavy metal contamination in road sweeping waste and bottom sediments of retention tanks. Sci. Total Environ. 749, 141511. https://doi.org/10.1016/j.scitotenv.2020.141511.

Nawrot, N., Wojciechowska, E., Matej-Łukowicz, K., Walkusz-Miotk, J., Pazdro, K., 2020b. Spatial and vertical distribution analysis of heavy metals in urban retention tanks sediments : a case study of Strzyza stream. Environ. Geochem. Health 8. https://doi.org/10.1007/s10653-019-00439-8.

Nishiuchi, S., Yamauchi, T., Takahashi, H., Kotula, L., Nakazono, M., 2012. Mechanisms for coping with submergence and waterlogging in rice. Rice 5, 2. https://doi.org/10.1186/1939-8433-5-2.

Obarska-Pempkowiak, H., Gajewska, M., Wojciechowska, E., Pempkowiak, J., 2015. Treatment wetlands for environmental pollution control. GeoPlanet https://doi.org/10.1007/978-3-319-13794-0 Springer.

Omwene, P.I., Öncel, M.S., Çelen, M., Kobya, M., 2018. Heavy metal pollution and spatial distribution in surface sediments of Mustafakemalpaşa stream located in the world's largest borate basin (Turkey). Chemosphere 208, 782–792. https://doi.org/10.1016/j.chemosphere.2018.06.031.

Packer, J.G., Meyerson, L.A., Skálová, H., Pyšek, P., Kueffer, C., 2017. Biological Flora of the British Isles: Phragmites australis. J. Ecol. 105, 1123–1162. https://doi.org/10.1111/1365-2745.12797.

Pathan, A.K., Bond, J., Gaskin, R.E., 2009. Sample preparation for SEM of plant surfaces. Mater. Today 12, 32–43. https://doi.org/10.1016/S1369-7021(10)70143-7.

Rezania, S., Taib, S.M., Md Din, M.F., Dahalan, F.A., Kamyab, H., 2016. Comprehensive review on phytotechnology: heavy metals removal by diverse aquatic plants species from wastewater. J. Hazard. Mater. 318, 587–599. https://doi.org/10.1016/j.jhazmat.2016.07.053.

Rezania, S., Park, J., Rupani, P.F., Darajeh, N., Xu, X., Shahrokhishahraki, R., 2019. Phytoremediation potential and control of Phragmites australis as a green phytomass: an overview. Environ. Sci. Pollut. Res. 26, 7428–7441. https://doi.org/10.1007/s11356-019-04300-4.

Rout, G., Das, P., 2003. Effect of metal toxicity on plant growth and metabolism, Review article effect of metal toxicity on plant growth and metabolism: I. Zinc. (doi: 10.1051/agro).

Rucińska-Sobkowiak, R., 2016. Water relations in plants subjected to heavy metal stresses. Acta Physiol. Plant. 38. https://doi.org/10.1007/s11738-016-2277-5.

Sarwar, N., Imran, M., Shaheen, M.R., Ishaque, W., Kamran, M.A., Matloob, A., Rehim, A., Hussain, S., 2017. Phytoremediation strategies for soils contaminated with heavy metals: modifications and future perspectives. Chemosphere 171, 710–721. https://doi.org/10.1016/j.chemosphere.2016.12.116.

Shaheen, S.M., Abdelrazek, M.A.S., Elthoth, M., Moghanm, F.S., Mohamed, R., Hamza, A., El-Habashi, N., Wang, J., Rinklebe, J., 2019. Potentially toxic elements in saltmarsh sediments and common reed (Phragmites australis) of Burullus coastal lagoon at North Nile Delta, Egypt: a survey and risk assessment. Sci. Total Environ. 649, 1237–1249. https://doi.org/10.1016/j.scitotenv.2018.08.359.

Shahid, M., Khalid, S., Abbas, G., Shahid, N., Nadeem, M., Sabir, M., Aslam, M., Dumat, C., 2015. Heavy Metal Stress and Crop Productivity. https://doi.org/10.1007/978-3-319-23162-4.

Shaltout, K.H., Al-sodany, Y., Eid, E.M., 2006. Biology of Common Reed Phragmites Review and Inquiry.

Shanker, A.K., Cervantes, C., Loza-Tavera, H., Avudainayagam, S., 2005. Chromium toxicity in plants. Environ. Int. 31, 739–753. https://doi.org/10.1016/j.envint.2005.02.003.

Shi, S.L., Lv, J.P., Liu, Q., Nan, F.R., Jiao, X.Y., Feng, J., Xie, S.L., 2018. Application of Phragmites australis to remove phenol from aqueous solutions by chemical activation in batch and fixed-bed columns. Environ. Sci. Pollut. Res. 25, 23917–23928. https://doi.org/10.1007/s11356-018-2457-5.

Singh, S., Parihar, P., Singh, R., Singh, V.P., Prasad, S.M., 2016. Heavy metal tolerance in plants: role of transcriptomics, proteomics, metabolomics, and ionomics. Front. Plant Sci. 6, 1–36. https://doi.org/10.3389/fpls.2015.01143.

Thakur, S., Singh, L., Wahid, Z.A., Siddiqui, M.F., Atnaw, S.M., Din, M.F.M., 2016. Plant-driven removal of heavy metals from soil: uptake, translocation, tolerance mechanism, challenges, and future perspectives. Environ. Monit. Assess. 188. https://doi.org/10.1007/s10661-016-5211-9.

Tomlinson, D.L., Wilson, J.G., Harris, C.R., Jeffrey, D.W., 1980. Problems in the assessment of heavy-metal levels in estuaries and the formation of a pollution index. Helgoländer Meeresun. 33, 566–575. https://doi.org/10.1007/BF02414780.

Vallius, H., Leivuori, M., 1999. The distribution of heavy metals and arsenic in recent sediments in the Gulf of Finland. Boreal Environ. Res. 4, 19–29.

Vymazal, J., 2016. Concentration is not enough to evaluate accumulation of heavy metals and nutrients in plants. Sci. Total Environ. 544, 495–498. https://doi.org/10.1016/j.scitotenv.2015.12.011.

Vymazal, J., Březinová, T., 2016. Accumulation of heavy metals in aboveground biomass of Phragmites australis in horizontal flow constructed wetlands for wastewater treatment: a review. Chem. Eng. J. 290, 232–242. https://doi.org/10.1016/j.cej.2015.12.108.

Weis, J.S., Glover, T., Weis, P., 2004. Interactions of metals affect their distribution in tissues of Phragmites australis. Environ. Pollut. 131. https://doi.org/10.1016/j.envpol.2004.03.006.

Wojciechowska, E., Waara, S., 2011. Distribution and removal efficiency of heavy metals in two constructed wetlands treating landfill leachate. Water Sci. Technol. 64, 1597–1606. https://doi.org/10.2166/wst.2011.680.

Wojciechowska, E., Rackiewicz, A., Nawrot, N., Matej-Łukowicz, K., Obarska-Pempkowiak, H., 2017. Investigations of heavy metals distribution in bottom sediments from retention tanks in the urbanized watershed. Annu. Set Environ. Prot. 19, 572–589.

Wojciechowska, E., Nawrot, N., Walkusz-Miotk, J., Matej-Łukowicz, K., Pazdro, K., 2019. Heavy metals in sediments of urban streams : contamination and health risk assessment of influencing factors. Sustain. 11, 563. https://doi.org/10.3390/su11030563.

Xie, Y., Hu, L., Du, Z., Sun, X., Amombo, E., Fan, J., Fu, J., 2014. Effects of cadmium exposure on growth and metabolic profile of bermudagrass [Cynodon dactylon (L.) Pers.]. PLoS One 9, 1–20. https://doi.org/10.1371/journal.pone.0115279.

Yadav, S.K., 2010. Heavy metals toxicity in plants: an overview on the role of glutathione and phytochelatins in heavy metal stress tolerance of plants. South African J. Bot. 76, 167–179. https://doi.org/10.1016/j.sajb.2009.10.007.

Yeh, N., Yeh, P., Chang, Y., 2015. Arti Fi Cial Fl Oating Islands for Environmental Improvement 47, 616–622. https://doi.org/10.1016/j.rser.2015.03.090.

Zaborska, A., 2014. Anthropogenic lead concentrations and sources in Baltic Sea sediments based on lead isotopic composition. Mar. Pollut. Bull. 85, 99–113. https://doi.org/10.1016/j.marpolbul.2014.06.013.